Supplemental Information for Gu et al.,

Supplemental Data:

Figure S1. Mapping actin binding domain (ABD) within dynamin

(A) Actin-cosedimentation assay in which dyn1 was expressed using coupled in vitro/transcription translation (IVT) assay followed by the actin co-sedimentation assay. Shown is a radiograph of ^{35}S labeled protein expressed in the assay, as well as Comassie stained gel showing presence of actin in the pellet fraction.

(B) Western blot analysis of recombinant dyn1 and purified actin. Cell lysates were used as a positive control for the presence of cortactin. Two higher order bands of dynamin in podocyte lysates are most likely post-translationally modified dynamin (e.g. phosphorylated dynamin).

(C and **D)** Scatchard analysis of dyn1^{WT} (C) and dyn1$^{\Delta PRD}$ (D) binding to 2.5 μM of F-actin. Increasing concentrations of dyn1 (free) were added to 2.5 μM of F-actin. After centrifugation at 150,000 x g proteins were separated on SDS-PAGE and bands were analyzed using densitometry.

(E) Actin-cosedimentation assays in which the GTPase domain (1-320) and the Middle domain (321-498) were expressed using coupled in vitro/transcription translation (IVT) assay followed by the actin co-sedimentation assay.

(F) Major actin-binding site is situated within amino acids 399-444. Dynamin lacking amino acids 399-444 was expressed using coupled in vitro/transcription translation (IVT) assay followed by the actin co-sedimentation assay. Deletion was placed within dyn1 and dyn2, and both mutants exhibited decreased ability to pellet with F-actin (compare lanes 2 and 4 for dyn1, and 6 and 8 for dyn2).

(G) Bar graphs depicting ability of dynΔ399-444 to pellet in the presence of F-actin. Dynamin distribution in each pool was expressed as a percentage of the total. Values shown are mean ± s.d. (n=3).

(H and **I)** Scatchard analysis of dyn1$^{K/E}$ (H) and dyn1$^{E/K}$ (I) binding to 2.5 μM of F-actin. Increasing concentrations of dyn1 (free) were added to 2.5 μM of F-actin. After centrifugation at 150,000 x g proteins were separated on SDS-PAGE and bands were analyzed using densitometry.

(J) Assembly activity of 5 μg dyn1^{WT}, dyn1$^{K/E}$, dyn1$^{K/A}$ and dyn1$^{E/K}$ assayed at 15, 75 and 150 mM NaCl. Comassie-blue-stained gel from a single representative assay (S: supernatant; P: pellet)

Figure S2. Mutations within the ABD do not alter endocytosis of transferrin or signaling by Rho type GTPases

(**A**) Clathrin-mediated endocytosis is not inhibited in cells expressing dynamin mutants with altered affinity for actin. HeLa cells were infected with different viruses as indicated in the figure. 10 min after addition of R-Tfn (red) cells were fixed and stained for dynamin (green) so that infected cells could be identified.

(**B**) Bar graph depicting the internalization of R-Tfn. The amount of internalized R-Tfn was accessed inside the cell (recycling endosomes), using ImageJ™ software. Values shown are mean ± s.d. for at least 100 cells.

(**C**) Immunoblot analysis of Rac1, Cdc42 and RhoA steady-state protein levels in cells expressing different dynamin mutants. Total amount of small GTPases was assessed. GAPDH was used as a loading control.

(**D**) Levels of active Rac1 and Cdc42 was assessed in a GST-PBD pull-down assay, whereas levels of active RhoA was assessed in a GST-RBD pull-down assay. Non-infected cells (Endo) served as control.

Figure S3. Direct dynamin-F-actin interactions are essential for organization of the actin cytoskeleton in podocytes

(**A**) Levels of dyn2 mRNA determined by RT-PCR. Endo, control podocytes not infected with lentiviruses. Scr, cells infected with lentiviruses expressing a scrambled oligo. S3-S5, cells infected with different shRNA constructs downregulating endogenous dyn2.

(**B**) Western blot analysis of dyn2 levels in cultured podocytes infected with lentiviruses expressing different shRNA constructs.

(**C**) Downregulation of dyn2 leads to dramatic decrease in F-actin in podocytes. Podocytes were infected with lentiviruses expressing the indicated shRNA constructs to downregulate dyn2, and cells were subsequently stained with rhodamine-phalloidin to visualize F-actin. Scr, podocytes infected with lentiviruses expressing a scrambled oligo.

(**D**) Expression of dyn1 did not rescue mRNA expression of dyn2 in podocytes. Levels of dyn2 mRNA determined by RT-PCR in cells expressing different dyn1 constructs. Podocytes were first infected with adenoviruses expressing dyn1 constructs ($dyn1^{WT}$, $dyn1^{E/K}$ and $dyn1^{K/E}$). 18 h post infection, cells were infected with lentivurus expressing shRNA construct S4, and dyn2 was downregulated for three days. Endo, control podocytes not infected with lentiviruses. ShRNA-S4 represents mRNA levels from podocytes in which dyn2 was downregulated and used as a control.

(**E**) Expression of dyn1 did not rescue protein expression of dyn2 in podocytes. Western blot analysis of dyn2 and dyn1 levels in cultured podocytes infected with lentiviruses expressing shRNA constructs S4 to downregulate dyn2, and different dyn1 constructs as indicated in the figure. Endo, control podocytes not infected with lentiviruses. GAPDH was used as loading control.

(**F**) Podocytes were first infected with adenoviruses expressing dyn1 constructs as indicated in the Figure. 18 h post infection, cells were infected with lentiviruses expressing shRNA construct S4, and dyn2 was downregulated for three days. Endo, control podocytes not infected with lentiviruses. Expression of dyn1 was visualized with anti-dyn1 antibodies (green), and F-actin was visualized using rhodamin-phalloidin (red).

Figure S4. Overexpression of ABD mutants alters organization of the actin cytoskeleton in clone 9 cells.

(**A** and **B**) Clone 9 cells were infected with adenoviruses expressing the indicated constructs, and cells were subsequently stained with anti-dynamin antibody (green) and rhodamin-phalloidin to visualize F-actin (red). Overxpression of $dyn1^{WT}$ did not alter overall organization of actin cytoskeleton in clone 9 cells (panel 2 in B). In contrast, expression of $dyn1^{E/K}$ resulted in increased number of stress fibers within the cell body (panel 3 in B). Similar phenotype was observed by expression of $dyn1^{\Delta PRD}$ (panel 1 in A) and double mutant $dyn1^{\Delta PRD/EK}$ (panel 3 in A). Expression of $dyn1^{K/E}$ (panel 4 in B), and $dyn1^{\Delta PRD/KE}$ (panel 2 in A) resulted in dramatic change in cell morphology, which was accompanied by the loss of defined stress fibers, and appearance of very thin stress fibers within the cell body.

Figure S5. Overexpression of ABD mutants alters organization of the actin cytoskeleton and cell motility

(**A)** Podocytes were infected with adenoviruses expressing the indicated constructs, and cells were subsequently stained with anti-paxillin antibody (green) and rhodamine-phalloidin (red). Overexpression of dyn1^{WT} did not alter overall organization of actin cytoskeleton in podocytes (panel 2). In contrast, expression of dyn1^{K44A} resulted in loss of focal adhesions within the cell body and formation of super-mature focal adhesions (blue arrows) in the membrane vicinity (panel 3). These changes resulted in loss of stress fibers within the cell body, and formation of cortical actin bundle in the membrane vicinity (F-actin). Overexpression of 'loss of function' dyn1$^{K/E}$ resulted in dramatic loss of focal adhesion within cell body, accompanied by the loss of stress fibers (panel 4). In addition, notice that actin phenotype in cells expressing 'loss of function' mutants is more similar to that of downregulation of dyn2 (Figure 2), than to expression of dyn1^{K44A}. Expression of 'gain of function' dyn1$^{E/K}$ resulted in increase in number of focal adhesions within the cell body (blue arrows in panel 5), in addition to an increase in number of stress fibers.

(**B** and **C**) Bar graphs depicting total F-actin (B) and number of focal adhesions (C). Data represent measurements of >200 cells and are plotted as ±s.d. (n=3). **P<0.01

(**D**) Cultured fully differentiated podocytes (1), infected with adenoviruses expressing dyn2^{WT} (2), and dyn2$^{K/E}$ (3). 18 hours post infection podocytes were stained with anti-dynamin antibody (green), and phalloidin for F-actin (red).

(**E**) Sequence alignments between amino acids of dyn2, dyn3 and dyn1.

(**F**) Western blot analysis of interactions between different dynamin mutants and endogenous cortactin. Anti-dynamin antibodies were used to immunoprecipitate cortactin from cell extracts

isolated from cells transiently expressing different dynamins (dyn1^{WT}, dyn1$^{K/E}$ and dyn1$^{E/K}$). GAPDH was used as a loading control. Mouse IgG and dyn1$^{\Delta PRD}$ were both used as a negative controls (lanes 1 and 5, respectively).

(**G**) Representative images of a scrape wound assay using cultured podocytes expressing either wild-type or mutant dynamins. The wound was generated 6 h post viral infection, and the cells were allowed to migrate for 48 h.

(**H**) Bar graph depicting podocyte motility as % wound closure in (G). Cells expressing dyn1^{K44A}, dyn1$^{K/A}$, dyn1$^{K/E}$ and dyn1$^{E/K}$ are impaired in motility. Data are displayed as mean ± s.d. (n=3).

Figure S6. Dynamin does not bind barbed ends

(**A**) Light microscopy analysis of the time-course of annealing of filaments fragmented with a syringe needle. Panels represent fluorescence micrographs. 1 μM polymerized actin was sheared five times through a 27 gauge needle. Samples were diluted into fluorescence buffer and prepared for microscopy at the indicated time points. Where indicated, the assay contained 0.5 μM dyn1 (4 and 5), and 200 μM GTPγS (5). The bar is 5 μm.

(**B**) Comassie stain of Gsn-F-actin complexes generated using different ratios of gelsolin and actin (G:A) as indicated in the figure. Samples were centrifuged at 150,000xg for 30 min at 22 °C in a Sorvall M120 centrifuge.

(**C**) Quantification of amount of F-actin in supernatant (S) or pellet (P) in experiment shown in (B).

(**D**) Dynamin cannot shift short actin filaments capped by the capping protein (CP) from supernatant to pellet in a centrifugation assay. Actin was polymerized in the presence of CP (CP1:A10) for 20

min. 16.5 μM CP-capped actin filaments were incubated with 1 μM dyn1 for 30 min. Subsequently, samples were centrifuged at 150,000 x g for 30 min at 22˚C.

(**E**) Quantification of number of cells expressing different dynamin constructs with barbed ends.

Supplemental Experimental Procedures:

Lentiviral Knockdown: Differentiated podocytes cannot be efficiently transiently tranfected with DNA. Thus, endogenous dyn2 was downregulated using lentiviruses. shRNA lentiviral plasmids were obtained from Sigma-Aldrich and were used to generate lentiviral transduction particles in HEK293T cells. A target set of 3 clones with pLKO.1<-puro as the parental vector were used, designated as S3, S4 and S5 with sequences:

S3 5' CCGGGCCCTTGAGAAGAGGCTATATCTCGAGATATAGCCTCTTCTCAAGGGCTTTTTG 3'

S4 5' CCGGGCCCGCATCAATCGTATCTTTCTCGAGAAGATACGATTGATGCGGGCTTTTTG 3'

S5 5' CCGGCCTAGTGGACATGACAATGAACTCGAGTTCATTGTCATGTCCACTAGGTTTTTG 3'

Lentiviral knockdown of mouse dyn2 was performed in differentiated mouse podocytes as per the protocol from the RNAi Consortium. Briefly, mouse podocytes were allowed to differentiate in 6 well dishes. 10 days into differentiation, the media was replaced with fresh medium containing 8 μg/ml polybrene followed by addition of 75 μl of each virus/well separately. The cells were incubated with the virus for 24 hours, after which the medium was replaced with fresh growth medium with or without 1.25 μg/ml puromycin. Selection was performed for 3-5 days after which cells were harvested to assay for knockdown efficiency using qPCR and Western Blot. In addition, changes in phenotype were also monitored using immunofluorescence.

Dynamin Rescue: Mouse podocytes were allowed to differentiate in 6 well dishes with or without coverslips. 10 days into differentiation, the cells were infected with adenoviral vectors containing $dyn1^{WT}$, $dyn1^{E/K}$, $dyn1^{K/E}$, $dyn1^{\Delta PRD}$, $dyn1^{\Delta PRD/KE}$ and $dyn1^{\Delta PRD/EK}$. After 18 hours infection, the serum free

medium containing the adenovirus was replaced with fresh media containing 8 μg/ml polybrene followed by addition of 75μl of shRNA-s4 per well. The cells were incubated with the virus for 24 hours, after which the medium was replaced with fresh growth medium without puromycin selection. Three days post infection, cells grown on coverslips were fixed for immunofluorescence experiments and cells grown in 6 well dishes without coverslips were used for Western blot and quantitative PCR experiments.

Western Blot: Cells grown in 6 well dishes were washed once with 1X PBS and scraped into 50μl of RIPA buffer containing protease inhibitor cocktail. The samples were centrifuged at 12,000xg for 20 min and supernatant collected. The protein concentration of the samples was assayed using the Bio-Rad protein assay reagent and equal concentrations of protein were subjected to SDS PAGE and Western transfer. Blots were probed with anti dyn1 antibody (VAM SV041), dyn2 antibody (Hudy II) and anti-GAPDH antibody was used as a loading control.

Quantitative PCR: Cells grown in 6 well dishes were washed once with 1X PBS and treated with TRIZOL® reagent to allow complete cell lysis. RNA was extracted from the cells as per the manufacturer's protocol. RNA was quantitated and cDNA synthesis was performed using the Protoscript™ First strand cDNA Synthesis Kit from New England BioLabs as per manufacturer's instructions. Quantitative PCR was performed on Stratagene's Mx3000P QPCR system using Brilliant® SYBR® Green QPCR Master Mix (Stratagene) using primers for dyn2:

Primer 1 (exon 1,2): forward 5' CGTGGGCCGGGACTTCCTTCC 3'

reverse 5' TTCCGCATATTCTGTTTTGG 3'

Primer 2 (exon 2,3): forward 5' CTTTTCCAAAACAGAATATGCGG 3'

reverse 5' CAAGTTCAACACGTGTGGTGAG 3'

Mouse GAPDH primers were used as control. Fold expression changes were calculated using the comparative CT method for relative quantification with the equation $2^{-\Delta CT}$ and data was graphed using either Excel or Prism Software.

Co-sedimentation experiments used to determine Kds: 2.5 μM polymerized F-actin was incubated with increasing concentrations of dyn1 in actin polymerization buffer. The mixture was centrifuged at 150,000 x g for 30 min at 22°C in 200 μl tubes in a Sorvall M120 centrifuge. Proteins in supernatants and pellets were solubilized in SDS sample buffer and subjected to SDS-PAGE. Polypeptides were visualized by Comassie blue staining, or transferred to PVDF membrane for Western blot analysis. Band intensities were quantified using Image J™ software (v1.4, National Institutes of Health, Bethesda, MD). Kds were calculated by a nonlinear regression/one site binding (hyperbola) and Scatchard analysis using Graph Pad Prism (v 4.03) for Windows (Graph Pad, San Diego, CA, USA).

Release of Gsn from the barbed ends: Gsn-F-actin complexes were generated by adding the indicated amount of Gsn into the polymerization buffer. 20 μM of Gsn-F-actin complexes (1G:A1000) were incubated for 30 min at RT with 0.2 μM dyn1 with or without 200 μM GTPγs, centrifuged at 150,000 x g for 30 min, and the resultant pellet and supernatant were analyzed by SDS-PAGE.

Visualization of annealing by light microscopy: Described in (Andrianantoandro et al., 2001). 1 μM of actin was polymerized for 20 min. F-actin was sheared by pushing 5 times through a 0.5-inch 27

gauge needle on a 1.0 ml tuberculin syringe at RT. Fragmented filaments were allowed to anneal for 7 seconds or 2 h before dilution into fluorescence buffer and adsorption to cover slips. Annealing reactions were terminated by 200-fold dilution into fluorescence buffer (0.2 M DTT, 25 μM imidazole, 25 μM KCl, 4 mM $MgCl_2$, 1 mM EGTA, 3 mM glucose, 0.5 % (w/v) methyl cellulose, 0.02 mg/ml catalase, 0.1 mg/ml glucose oxidase). Rhodamine-phalloidin was added and filaments were adsorbed to covers slips coated with poly-L-lysine and imaged by Zeiss LSM 5 PASCAL laser scanning microscope (40x objective) and recorded with a Hamamatsu ORCA CCD camera. Measurement of filament length was carried out with Zeiss LSM image browser version 4,2,0,121 from Carl Zeiss. Lengths of 300-500 filaments per time experimental condition were measured, and calculated an average length. When indicated 0.5 μM of dyn1 and 200 μM GTPγS were added in the assay.

Visualization of F-actin crosslinking by light microscopy: Described in (Schafer et al., 2002): 5 μM of preassembled Gsn-F-actin complexes (G1:A1000) were incubated with 1 μM dyn1 in a polymerization buffer for 30 min at RT. When indicated 200 μM GTPγS was added to the assay. Reactions were terminated by 100-fold dilution into fluorescence buffer as described above containing rhodamine-phalloidin. Images were captured with a Zeiss LSM 5 PASCAL laser scanning microscope (10x objective).

Solution based actin polymerization:

1. Using actin seeds and CP-capped filaments: Experiments were performed as described in detail in (Fujiwara et al., 2009). Mouse recombinant CP, actin seeds and pyrine-labeled actin were all

generous gifts from Fujiwara Ikuko and John A Hammer III (Laboratory of Cell Biology, NIHBI/NIH, Bethesda, MD). CP was purified as described in detail in (Remmert et al., 2009). Mg-ATP-actin monomers were polymerized in KMEI buffer (50 mM KCl, 10 mM $MgCl_2$, 10 mM EGTA, 100 mM imidazole, pH 7.0) for 1 h. Actin 'seeds' were generated by polymerizing 8 μM Mg-ATP G-actin at room temperature for 1 h and then vortexing aliquots for 20 s immediately before addition to the assay. This sheared F-actin was added to the assay at a final concentration of 0.8 μM. When indicated, mouse CP was added at a final concentration of 5 nM for 5 min at RT. 0.2 μM of dyn1 was incubated with 0.8 μM CP-capped or uncapped actin seeds in presence or absence of 300 μM GTPγS for 30 min at 22°C. Assay was initiated by addition of 2 μM pyrene-labeled G-actin (20% labeled) which was previously converted to Mg-ATP-actin in ME buffer (1 mM EGTA, 0.1 mM $MgCl_2$). Pyrene fluorescence was monitored with excitation at 365 nm and emission at 407 nm using a SpectraMax M2E (Molecular Devices, Sunnyvale, CA).

1. Using geloslin-capped filaments: Assays were performed as described in detail in (Moseley et al., 2006) with the modification that we used preassembled Gsn-F-actin complexes. 5 μM Gsn-F-actin complexes (G1:A1000) were incubated with 0.2 μM dyn1 with or without 200 μM GTPγS. Reaction was initiated by addition of 0.5 μM pyrene-G-actin (10% labeled) obtained from Cytoskeleton, and pyrene-actin fluorescence was followed using a SpectraMax M2E (Molecular Devices, Sunnyvale, CA). Excitation and emission wavelengths were 365 and 407 nm, respectively.

Fluorimeter-based F-actin deploymerization assay: Described in (Barkalow et al., 1996; Pruyne et al., 2002): 10μM pyrene-actin (10% pyrene-labeled, Cytoskeleton Inc.) was polymerized in the presence of gelsolin (G1:A200 and G1:A1000) as described above. The Gsn-F-actin was diluted to 3.3 μM in

the actin polymerization buffer containing 0.1 μM dynamin in the presence or absence of 100 μM GTPγS. To start the assay, Gsn-F-actin was further diluted to 0.33 μM in actin polymerization buffer, and pyrene-actin fluorescence was followed using a KS50B spectrofluorimeter (Perkin-Elmer). Excitation and emission wavelengths were 366 and 386 nm, respectively.

Electron microscopy and negative staining of actin filaments: Performed as described in (Hartwig and Stossel, 1981). Briefly, 25 μM Gsn-F-actin (G1:A100 for dynamin rings, and G1:A1000 for bundling experiments) was generated as described above. Phallacidin (1μM) was added to stabilize filaments and incubated for another 20 minutes at RT. Recombinant dynamin was added at a dynamin:actin ratio of 1:5 and incubated for 60 min. Formvar coated, glow-discharged 200 mesh copper grids were put onto a drop of protein mix (~50-100 μg/ml) for 1 minute, excess fluid removed, and washed quickly in polymerization buffer with phallacidin. The grid was stained in two drops of 2% uranyl acetate for approximately 30 seconds, excess fluid removed, and air-dried on filter paper.

Electron microscopy of podocyte cytoskeletons: Experiments were performed as described in detail in (Schliwa et al., 1981). Briefly, podocytes were grown on glass coverslips 5 mm in diameter and cytoskeletons revealed by treating the cells with 0.75% Triton X-100 in PHEM buffer containing 1 μM phallacidin. Cytoskeleton were washed in PHEM and fixed in 0.5% glutaraldehyde in PHEM for 10 min. Coverslips containing cytoskeleton were fixed, blocked and subsequently stained. Dynamin antigenic sites were stained using a combination of two monoclonal anti-dynamin antibodies (mouse monoclonal VAM-SV041 and mouse monoclonal hudy1). Paxillin antigenic sites were detected using rabbit polyconal anti-paxillin antibody. Anti-mouse IgG-coated gold (10 nm) were used to detect

dynamin, and anti-rabbit IgG-coated gold (5 nm) were used to detect paxillin. Samples stained with only secondary antibodies were used as control.

Subcellular-fractionation experiments: Performed as described in (Watts and Howard, 1992; Yamamoto et al., 2001). Differentiated podocytes previously infected with appropriate adenoviruses were grown on 6 well dishes. Cells were briefly washed with 1XPBS. Cells were scraped and placed into ice cold lysis buffer containing 1% Triton X-100, 10 mM imidazole, 10 mM EGTA, 40 mM KCl, 0.01 mM PMSF, pH=7.2. Samples were centrifuged at 15,900 x g for 2 min to isolate actin bundles (Triton X-100 insoluble fraction, low speed pellet, (LSP)). The Triton X soluble fraction was removed and further centrifuged at 366,000 X g for 20 min to separate unbundled F-actin (high speed pellet (HSP)) from soluble globular actin (high speed supernatant, (HSS)). Equal volumes were separated by SDS-PAGE, transferred to PVDF membranes and immunoblotted with anti–actinin 4 antibody and anti-actin antibodies (Sigma).

Immunoprecipitation and immunoblotting: Mouse podocytes expressing wild-type or each dyn1 mutant on 10 cm dishes were washed one time with cold phosphate-buffered saline (PBS) and then lysed in 1 ml of cold lysis buffer (25 mM HEPES, pH 7.5, 150 mM NaCl, 10% glycerol, 1% NP-40, 10 mM $MgCl_2$, 1mM EDTA, 1 mM PMSF, calpain inhibitor and protease inhibitors). Lysates were clarified by centrifugation in a microcentrifuge for 10 min at 4˚C, and then incubated with anti-dynamin antibody VAM-SV041 for 1.5 h on ice. Protein G-Sepharose (Invitrogen) was added and incubated for 30 min, and immunoprecipitates were washed two times in cold lysis buffer, and samples were subsequently boiled in SDS-sample buffer, loaded on 8% SDS-polyacrylamide gels and separated by

electrophoresis. Proteins were electrophoretically transferred to PVDF (Millipore) membranes. Membranes were blocked in PBS containing 0.1% Tween-20 and 5% non-fat dry milk and immunoblotted using mouse monoclonal anti-dynamin and anti-cortactin antibody. A sample (4%) of each total cell lysate was analyzed directly by immunoblotting using the same antibodies. Detection of primary antibodies was performed using horseradish peroxidase-conjugated goat anti-mouse IgG followed by SuperSignal Chemiluminescence (Thermo Scientific).

Free barbed ends: The number of barbed ends in podocytes was examined as described in (Chan et al., 1998). Mouse podocytes expressing different dynamin constructs were serum starved for 3 hours and then stimulated with a final concentration of 5 nM EGF (Molecular Probes) for 5 min. Of note, by altering EGF incubation time we have determined that 5 min stimulation gave the best results in cultured podocytes. Biotin G-actin (Cytoskeleton) was reconstituted in buffer containing 1 mM Hepes, pH 7.5, 0.2 mM $MgCl_2$, and 0.2 mM ATP and was subsequently centrifuged at 250,000 g for 30 min to remove aggregates. Cells were permeabilized in the presence of 0.45 mM biotin G-actin in permeabilization buffer (20 mM Hepes, pH 7.5, 138 mM KCl, 4 mM $MgCl_2$, 3 mM EGTA, 0.2 mg / ml of saponin, 1 mM ATP, 1 % BSA) for 45 sec and the reaction was stopped by adding permeabilization buffer without saponin and BSA. Cells were fixed in 4 % PFA in cytoskeleton stabilization buffer (5 mM KCl, 137 mM NaCl, 4 mM $NaHCO_3$, 0.4 mM KH_2PO_4, 1.1 mM Na_2HPO_4, 2 mM $MgCl_2$, 5 mM Pipes, 2 mM EGTA, 5.5 mM Glucose) for 30 min, followed by 10 min incubation in 0.1 M glycine in cytoskeleton stabilization buffer. Fixed cells were incubated with rhodamine-conjugated anti-biotin antibody (Jackson ImmunoResearch Laboratories) for 1 hr. For quantitation, cells images in fields randomly chosen were acquired using Zeiss LSM 5 PASCAL laser scanning microscope (40x

objective). Cells with barbed ends were counted. To determine the size of biotin G-actin incorporated into actin filaments, image processing was performed by using Zeiss LSM 5 Image Browser Version 4,2,0,121 (Carl Zeiss), Photoshop 7.0 (Adobe Systems) and Image J software (National Institutes of Health, Bethesda, MD). Data were further analyzed using GraphPad Prism (v 4.03) for Windows (GraphPad Software, San Diego, CA) to perform statistical analysis using two-tailed unpaired t-tests. Based on this analysis *$p<0.05$, **$p<0.01$ and $p>0.05$ is considered not significant (n.s).

Supplemental References:

Andrianantoandro, E., Blanchoin, L., Sept, D., McCammon, J.A. and Pollard, T.D. (2001) Kinetic mechanism of end-to-end annealing of actin filaments. *J Mol Biol*, **312**, 721-730.

Barkalow, K., Witke, W., Kwiatkowski, D.J. and Hartwig, J.H. (1996) Coordinated regulation of platelet actin filament barbed ends by gelsolin and capping protein. *J Cell Biol*, **134**, 389-399.

Chan, A.Y., Raft, S., Bailly, M., Wyckoff, J.B., Segall, J.E. and Condeelis, J.S. (1998) EGF stimulates an increase in actin nucleation and filament number at the leading edge of the lamellipod in mammary adenocarcinoma cells. *J Cell Sci*, **111 (Pt 2)**, 199-211.

Fujiwara, I., Remmert, K. and Hammer, J.A., 3rd. (2009) Direct observation of the uncapping of capping protein-capped actin filaments by CARMIL homology domain 3. *J Biol Chem*, **285**, 2707-2720.

Hartwig, J.H. and Stossel, T.P. (1981) Structure of macrophage actin-binding protein molecules in solution and interacting with actin filaments. *J Mol Biol*, **145**, 563-581.

Moseley, J.B., Maiti, S. and Goode, B.L. (2006) Formin proteins: purification and measurement of effects on actin assembly. *Methods Enzymol*, **406**, 215-234.

Pruyne, D., Evangelista, M., Yang, C., Bi, E., Zigmond, S., Bretscher, A. and Boone, C. (2002) Role of formins in actin assembly: nucleation and barbed-end association. *Science*, **297**, 612-615.

Remmert, K., Uruno, T. and Hammer, J.A., 3rd. (2009) Purification of capping protein using the capping protein binding site of CARMIL as an affinity matrix. *Protein Expr Purif*, **67**, 113-119.

Schafer, D.A., Weed, S.A., Binns, D., Karginov, A.V., Parsons, J.T. and Cooper, J.A. (2002) Dynamin2 and cortactin regulate actin assembly and filament organization. *Curr Biol*, **12**, 1852-1857.

Schliwa, M., van Blerkom, J. and Porter, K.R. (1981) Stabilization and the cytoplasmic ground substance in detergent-opened cells and a structural and biochemical analysis of its composition. *Proc Natl Acad Sci U S A*, **78**, 4329-4333.

Watts, R.G. and Howard, T.H. (1992) Evidence for a gelsolin-rich, labile F-actin pool in human polymorphonuclear leukocytes. *Cell Motil Cytoskeleton*, **21**, 25-37.

Yamamoto, M., Hilgemann, D.H., Feng, S., Bito, H., Ishihara, H., Shibasaki, Y. and Yin, H.L. (2001) Phosphatidylinositol 4,5-bisphosphate induces actin stress-fiber formation and inhibits membrane ruffling in CV1 cells. *J Cell Biol*, **152**, 867-876.

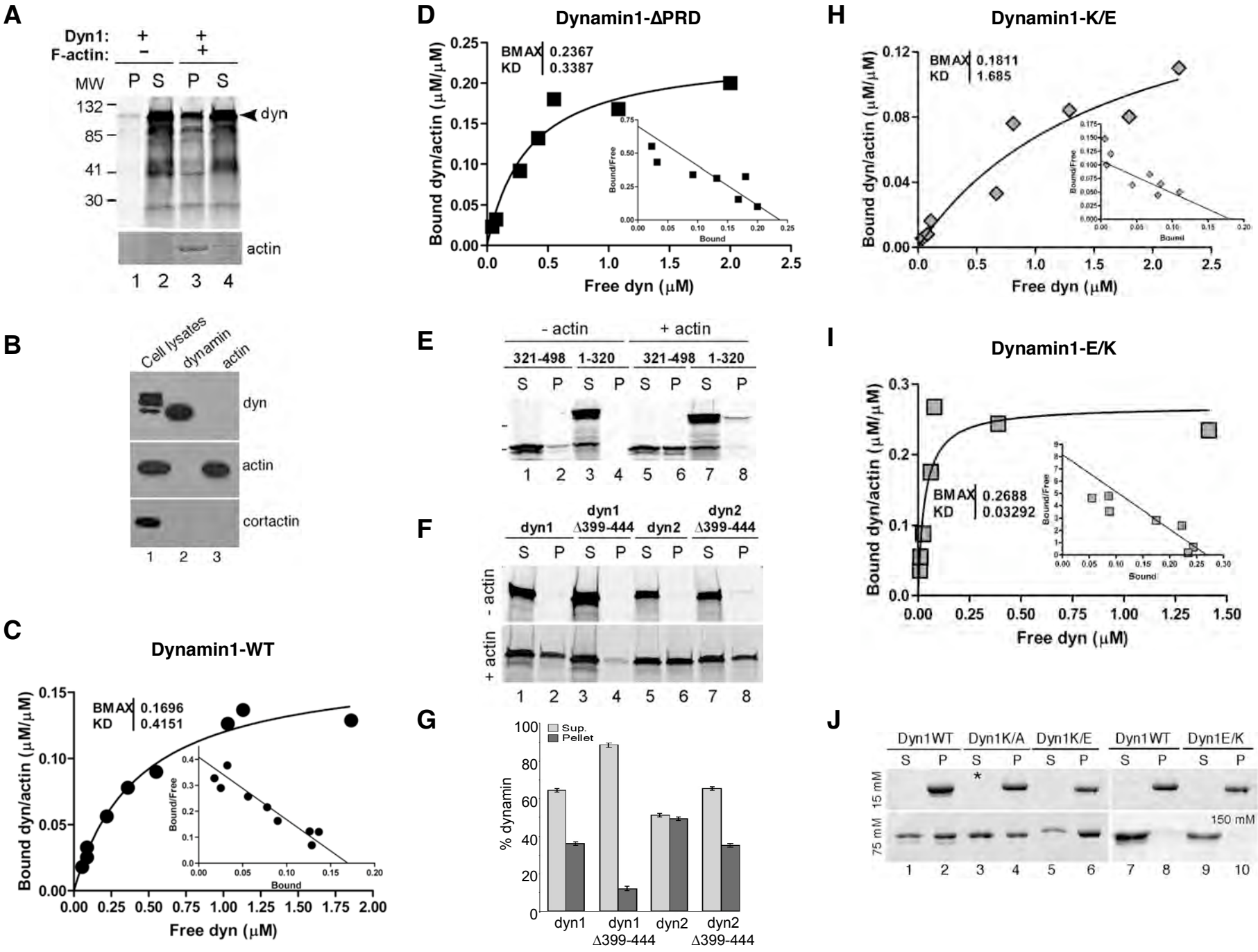

Figure S1., Gu et al.

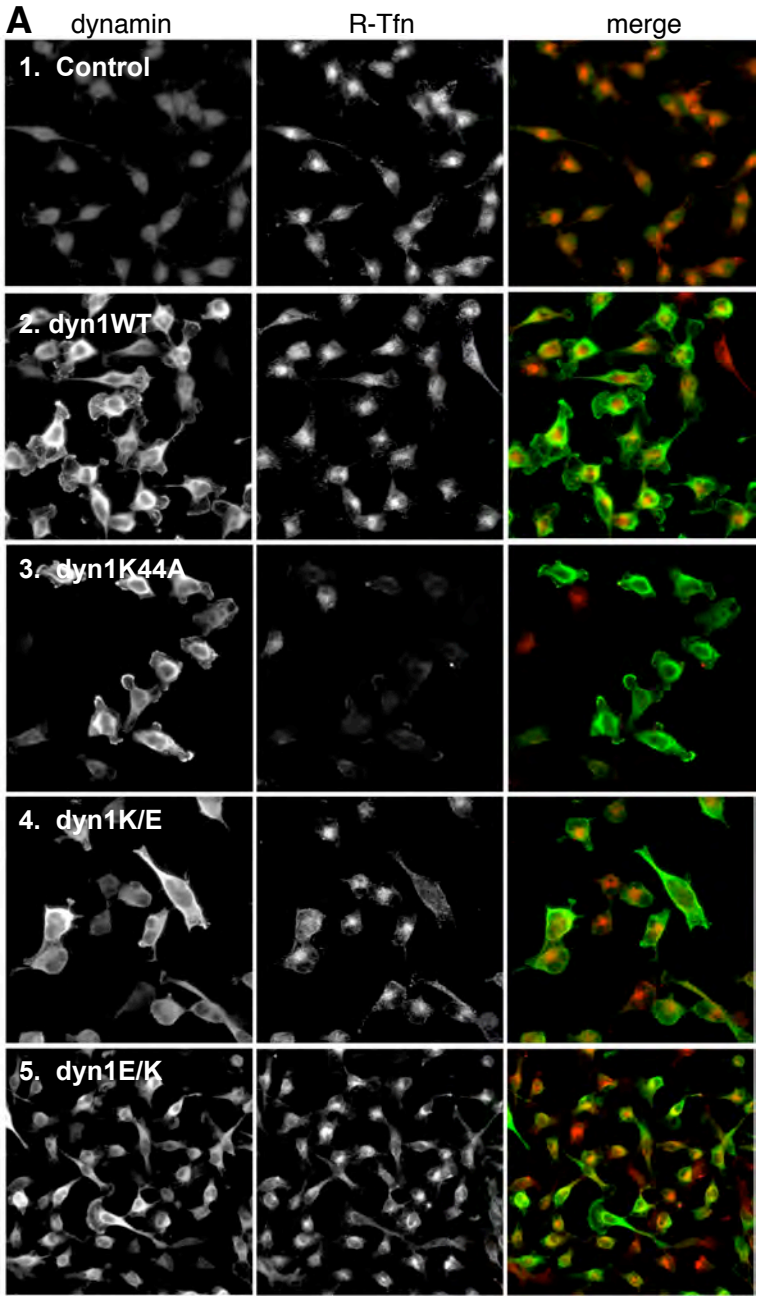

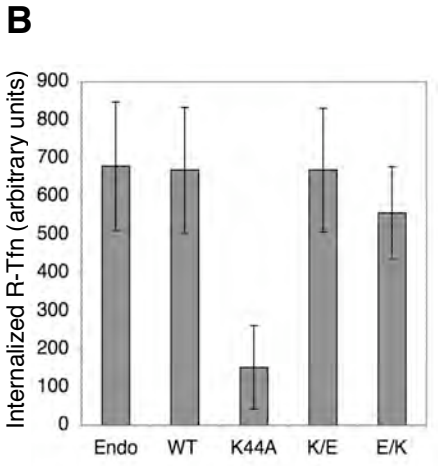

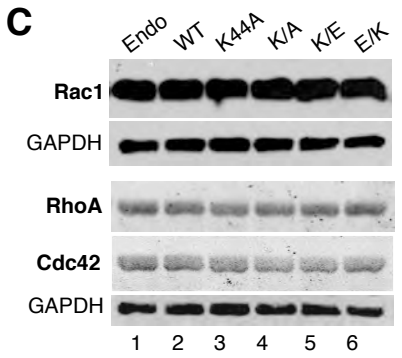

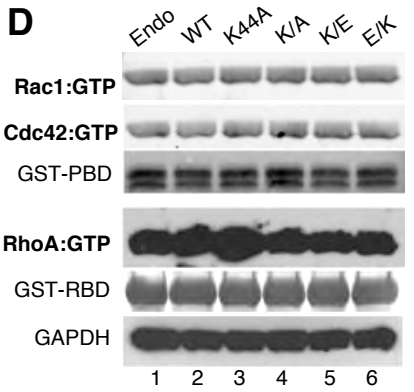

Figure S2., Gu et al.,

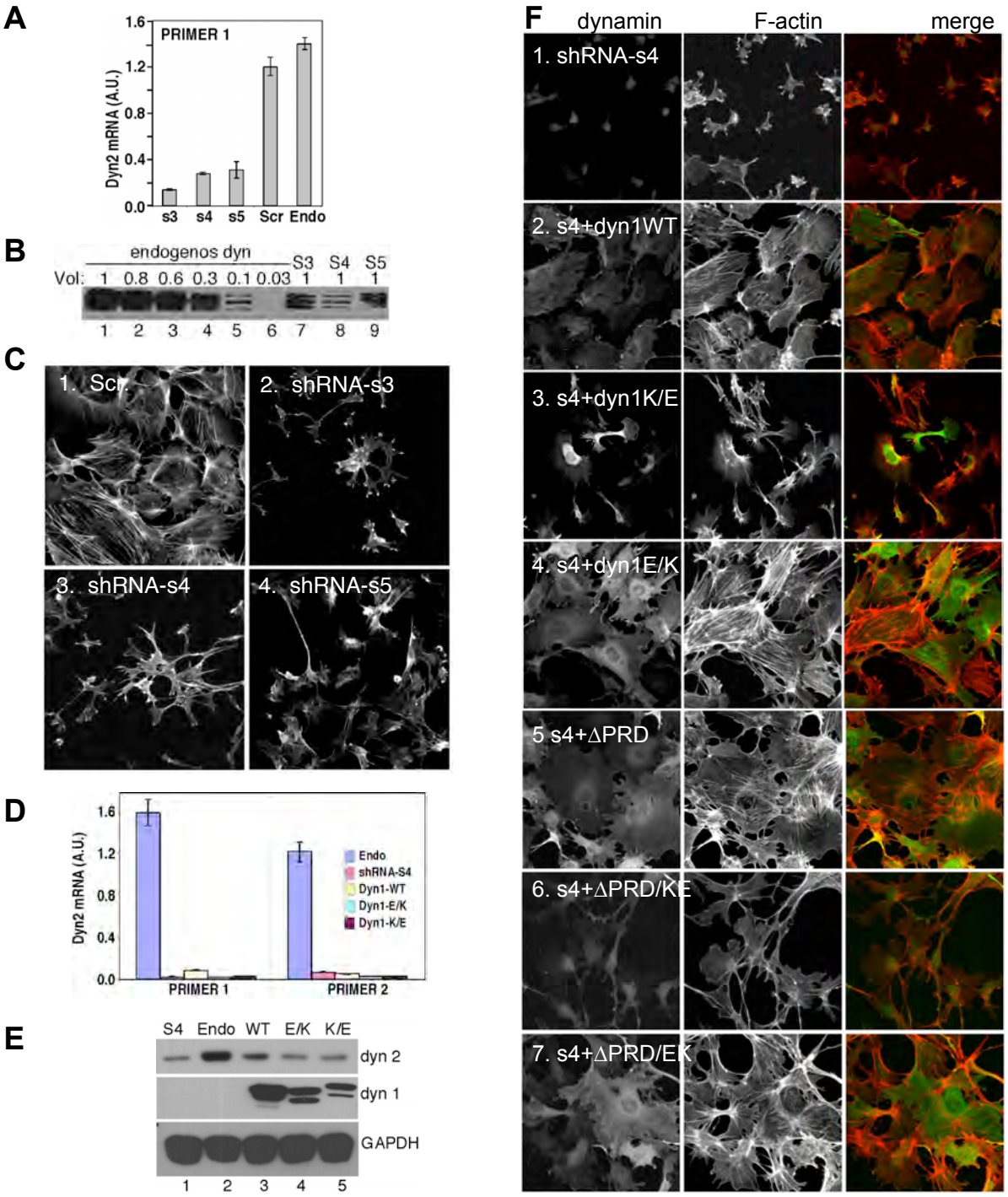

Figure S3., Gu et al.,

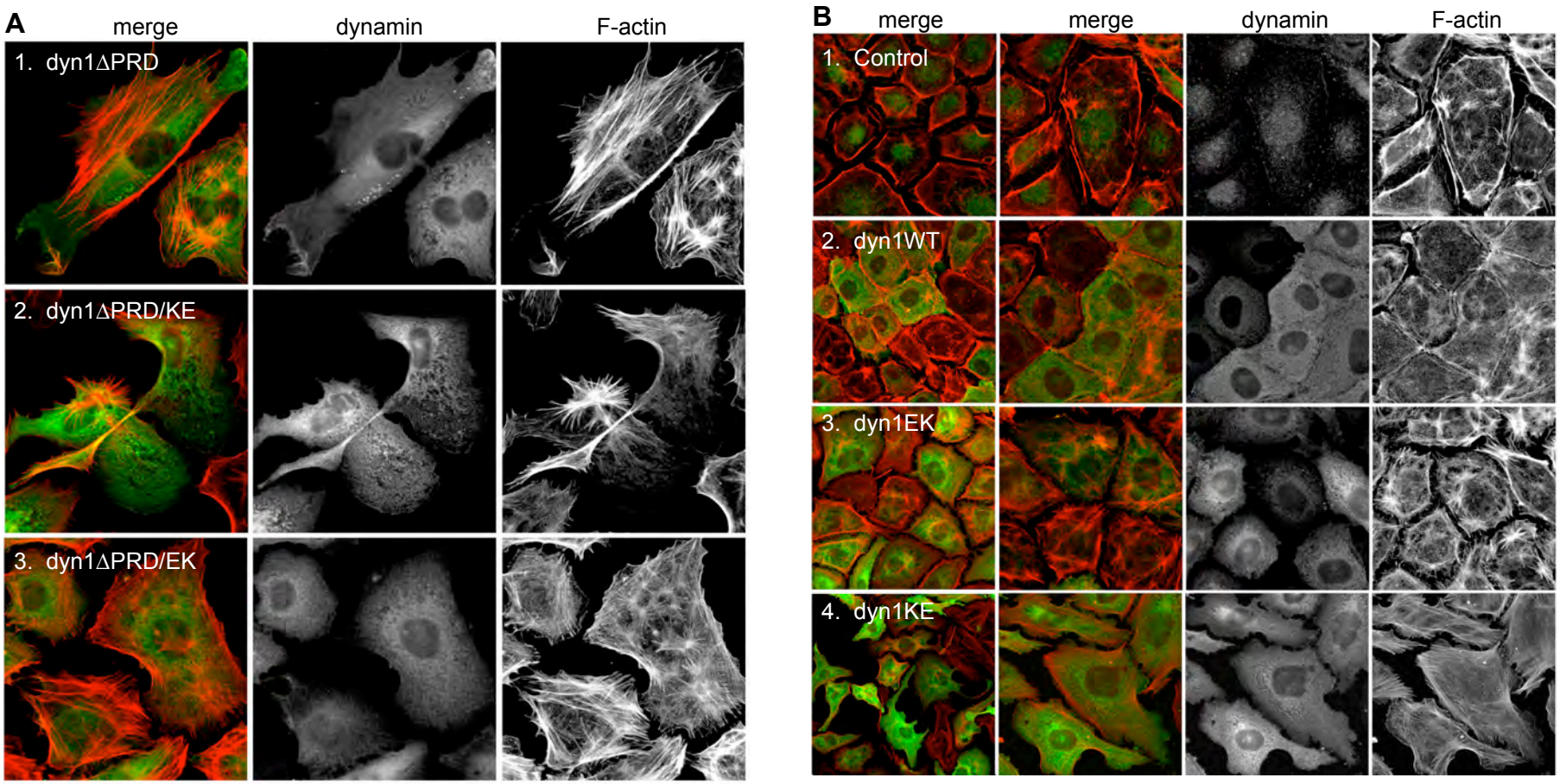

Figure S4., Gu et al.,

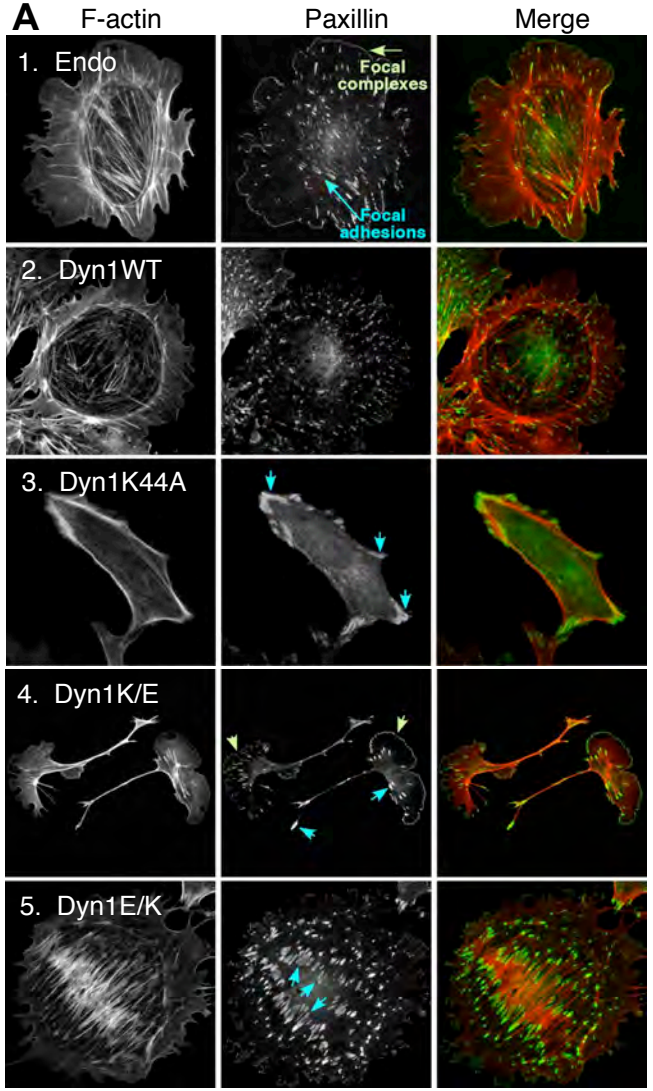

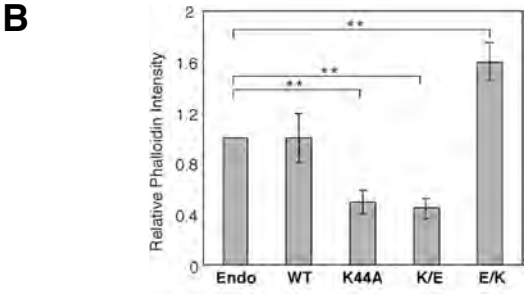

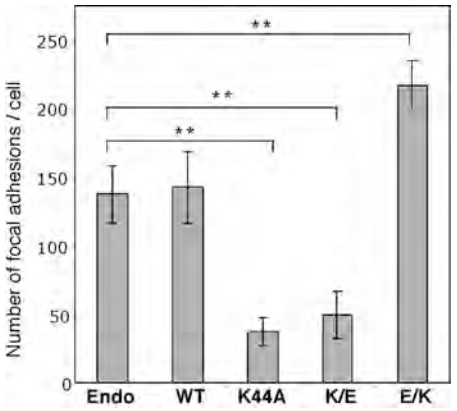

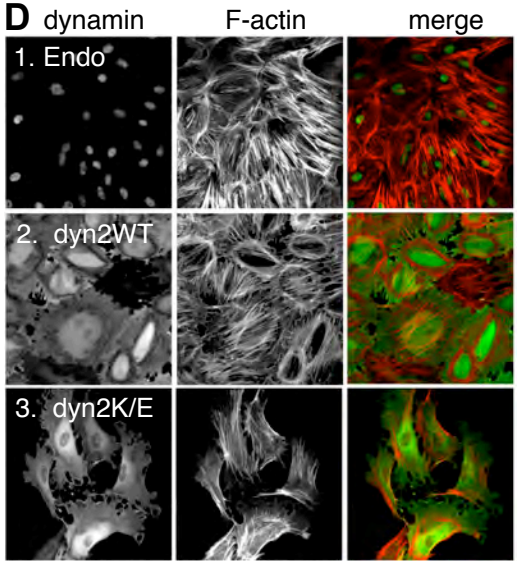

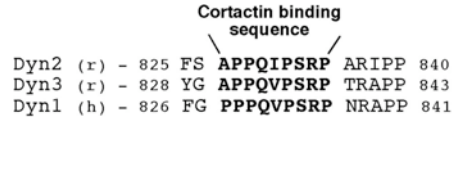

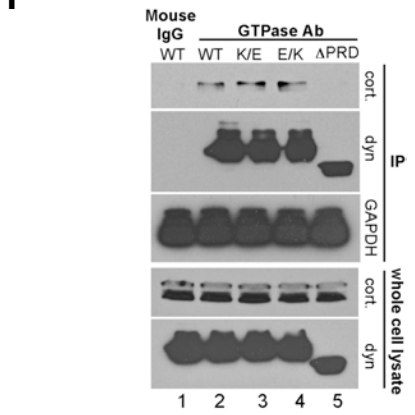

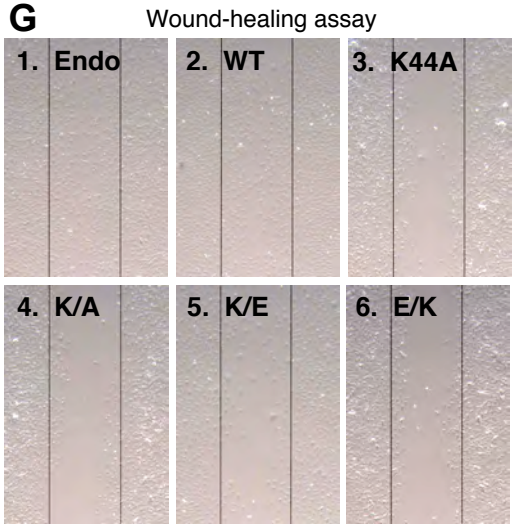

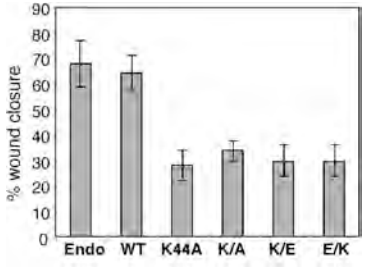

Figure S5.,
Gu et al.,

A

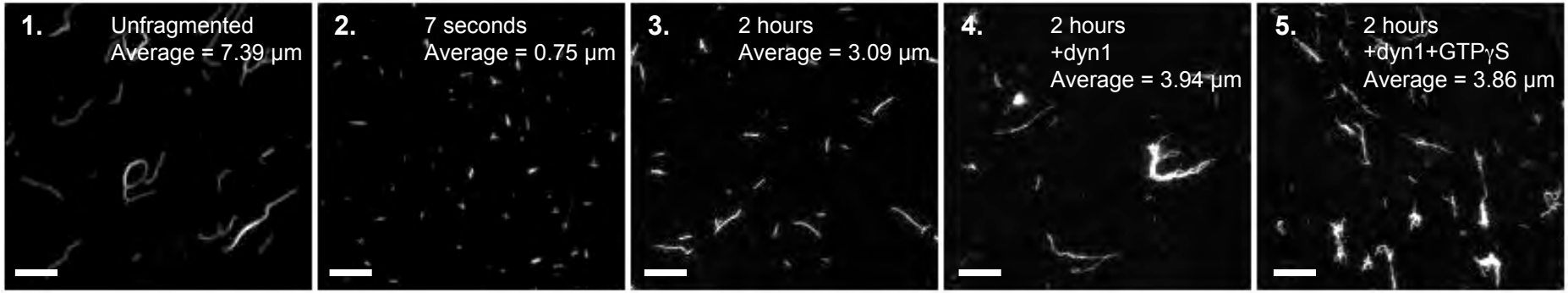

B

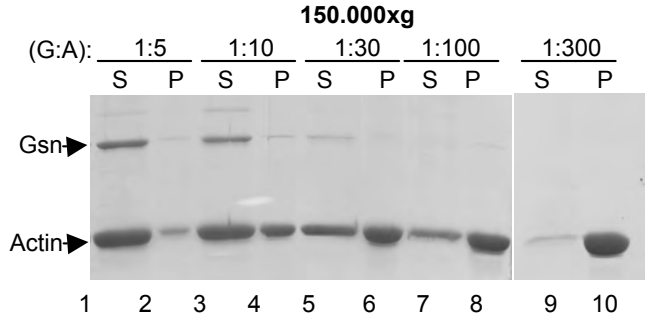

C

Gsn:actin	S : P
1 : 5	95 : 5
1 : 10	70 : 30
1 : 30	45 : 55
1 : 100	35 : 65
1 : 300	8 : 92

D

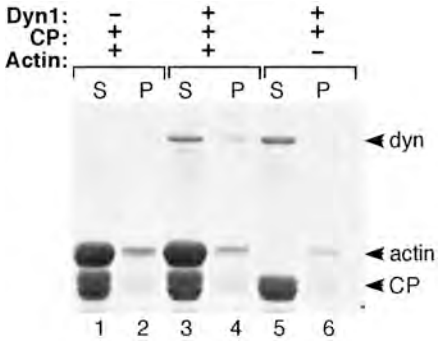

E

Dyn1	EGF	% cells with barbed ends
Endo	-	0.5
Endo	+	4.9
WT	+	4.6
K/E	+	0.65
E/K	+	6.5

Figure S6., Gu et al.